The Cryosphere Discuss., 9, 4925–4948, 2015
www.the-cryosphere-discuss.net/9/4925/2015/
doi:10.5194/tcd-9-4925-2015

The Cryosphere Discussions
Open Access

Time forecast of a break-off event from a hanging glacier

J. Faillettaz[1], M. Funk[2], and M. Vagliasindi[3]

[1]3G, UZH, University of Zürich, Zürich, Switzerland
[2]VAW, ETHZ, Zürich, Switzerland
[3]Fondazione Montagna Sicura, Courmayeur, Aosta Valley, Italy

Received: 5 August 2015 – Accepted: 1 September 2015 – Published: 17 September 2015

Correspondence to: J. Faillettaz (jerome.faillettaz@geo.uzh.ch)

Published by Copernicus Publications on behalf of the European Geosciences Union.

Abstract

A cold hanging glacier located on the south face of the Grandes Jorasses (Mont Blanc, Italy) broke off on the 23 and 29 September 2014 with a total estimated ice volume of 105 000 m^3. Thanks to very accurate surface displacement measurements taken right up to the final break-off, this event could be successfully predicted 10 days in advance, enabling local authorities to take the necessary safety measures. The break-off event also confirmed that surface displacements experience a power law acceleration along with superimposed log-periodic oscillations prior to the final rupture. This paper describes the methods used to achieve a satisfactory time forecast in real time and demonstrates, using a retrospective analysis, their potential for the development of early-warning systems in real time.

1 Introduction

Rockfalls, rock instabilities due to permafrost degradation, landslides, snow avalanches or avalanching glacier instabilities are gravity-driven rupture phenomena occurring in natural heterogeneous media. Such events have a potential to cause major disasters, especially when they are at the origin of a chain of processes involving other materials such as snow (snow avalanche), water (flood) and/or debris (mudflow). The reliable forecasting of such catastrophic phenomena combined with a timely evacuation of the endangered areas is often the most effective way to cope with such natural hazards. Unfortunately, accurate time prediction of such events remains a somewhat daunting task as (i) natural materials are heterogeneous, (ii) the heterogeneity is difficult to quantify and measure, and (iii) the rupture is a non-linear process involving such heterogeneities. Although often located in a remote high-mountain environment, avalanching glacier instabilities offer an interesting starting point for investigating early-warning perspectives of break-off events, as a glacier consists of a unique material (ice) lying on well-defined bedrock. This relative simplicity of the system allows the focus to be placed on the rupture processes leading to the initiation of the instability. Recently, considerable efforts in monitoring, analyzing and modeling such phenomena have led to significant advances in understanding the destabilization process and in improving early-warning perspectives (Faillettaz et al., 2015).

In general, it is possible to distinguish three types of avalanching glacier instabilities according to the thermal properties of their ice/bedrock interface (Faillettaz et al., 2011b, 2012, 2015). If temperate or polythermal, the presence of liquid water in the glacier plays a key role in the initiation and the development of the instability as its presence influences the basal properties of the ice/bedrock interface (diminution of friction, lubrication or loss of support). In such cases, several preliminary conditions to be fulfilled can be identified, but an accurate time forecast of an impending break-off event is still far from being possible. If the ice/bed interface is partly temperate, the presence of melt water may reduce the basal resistance, which promotes the instability. No clear and easily detectable precursory signs are known in this case, and the only way to infer any potential instability is to monitor the temporal evolution of the thermal regime. If the ice/bedrock is cold, glaciers are entirely frozen to their bedrock. This situation appears in the case of high altitude hanging glaciers located entirely in accumulation zone. The snow accumulation is mostly compensated by periodic break-off of ice chunks (Pralong and Funk, 2006), occurring once a critical point in glacier geometry is reached. The instability results from the progressive accumulation of internal damage due to an increasing stress regime caused by glacier thickening. In this case, the rupture occurs within the ice, typically a few meters above the bedrock. The maturation of the rupture was shown to be associated with a typical time evolution of both surface velocities (Faillettaz et al., 2008) and passive seismic activity (Faillettaz et al., 2011a). This characteristic time evolution can theoretically be used to predict the occurrence of a catastrophic event. This was done a posteriori with data obtained prior to the 2005 break-off of the Weisshorn glacier.

In this context, the Whymper glacier, a cold hanging glacier located at the Grandes Jorasses (Mont Blanc, Alps, Italy), already broke off several times in the past, leading

TCD
9, 4925–4948, 2015

to major ice avalanches that occasionally reached as far as the valley. In autumn 2008, the glacier recovered its previous critical geometry from the year 1998 and a crevasse opened in the lower part of the tongue, prompting the local authorities to initiate a monitoring program to enable a time forecast of the expected break-off event. The glacier finally broke off causing no damage in autumn 2014, after more than 5 years of monitoring. The break-off was successfully predicted 2 weeks in advance.

The aim of this paper is to confirm the validity of the time forecast procedure first developed in 2005 on the Weisshorn glacier and to apply it here in real time.

After describing the glacier and the monitoring system installed on the glacier, we analyze the time evolution of the surface displacement measurements in the context of a time forecast procedure. While comparing this break-off event with the Weisshorn glacier break-off event of 2005 we discuss the results obtained, with the goal of improving the understanding of this phenomenon.

2 Grandes Jorasses glacier

2.1 Study site

The Whymper glacier (Fig. 1) is located on the south face of the Grandes Jorasses (Mont Blanc massif, Italy) between 3900 and 4200 m a.s.l. (Fig. 1). This very steep cold hanging glacier lies above the village of Planpincieux and the Italian Val Ferret, a famous and highly frequented tourist destination both in winter and summer. Historical data and morphological evidence indicate that the glacier experienced recurrent break-off events that can be dangerous, particularly in winter, when the initial ice avalanche can drag snow in its path. This hanging glacier periodically broke off in the past leading to large avalanches that flowed down into the valley.

2.2 Break-off event history

The glacier broke off several times during last 100 years. Some of these events have been observed and reported:

- On 21 December 1952, after an intensive snowfall period, a huge avalanche was released below the Grandes Jorasses which destroyed a 200 year old forest and blocked the bottom of the Val Ferret over a distance of more than 1 km. The avalanche volume was estimated at more than 1 000 000 m^3. It is not clear whether the snow avalanche was triggered by an ice avalanche from the Whymper glacier.
- In August 1993 and July 1996, the glacier released ice avalanches of 80 000 and 24 000 m^3, respectively. These ice avalanches did not reach the valley.
- The last major break-off event occurred in the night of 31 May to 1 June 1998. Almost the entire Whymper glacier (around 150 000 m^3) broke off at one time and the triggered ice avalanche reached the bottom of the valley, fortunately without causing damage.

In the following years, the hanging glacier has progressively re-formed, as it is located in an accumulation area. Ten years later, in 2008, the glacier almost recovered its 1998 geometry. In autumn 2008 a crevasse opened at the lower part of the glacier, prompting the local authorities to initiate a monitoring program.

2.3 Present monitoring: 2009–2014

The survey primarily consisted of surface displacement measurements with an automatic total station and GPS as well as close-range photogrammetry. Two reflectors set on the rock on both sides of the glacier were used as reference, and several reflectors mounted on stakes were directly drilled into the ice, so that their exact positions could

TCD
9, 4925–4948, 2015

be monitored. Because of instrument problems, the seismic activity unfortunately could not be monitored as initially planned.

Starting in 2010, surface displacements were continuously recorded at several stakes at 2 h intervals (if the prisms were visible, i.e., in good weather conditions) with the aim to detect an impending ice avalanche in a timely manner (Margreth et al., 2011). Using the same correction technique as described by Faillettaz et al. (2008), the surface displacements could be determined with an accuracy better than 1 cm, allowing surface velocities to be inferred.

In parallel to the monitoring program, a safety concept for the valley floor was developed considering several scenarios of falling ice volumes. The different ice avalanche scenarios were simulated using the 2-dimensional calculation model RAMMS. The necessary safety measures were defined according to the local avalanche danger level and the potential volume of a break-off event (Margreth et al., 2011).

2.4 The 2014 break-off event

From 2010 on, surface displacements were surveyed without interruption. The Whymper glacier finally broke off with an estimated ice volume of same order of magnitude as the 1998 event (about 105 000 m^3). Contrary to the 1998 event, the glacier broke off in two events on 23 and 29 September 2014, without reaching the valley (Fig. 1). At the final break-off, 4 reflectors were still active, 2 of them in place for more than 2 years. Despite poor weather conditions between the 16 and 21 September, the monitoring was operational up to the final break-off. By chance, there was at least one reflector on each part of the glacier (one on each unstable part and one on the stable part, Fig. 1). Note that contrary to previous studies, these constitute the first accurate surface displacement measurements on a hanging glacier up to the break-off event.

TCD
9, 4925–4948, 2015

3 Results

Figure 2 shows the corrected surface displacements and Fig. 3 the associated derived surface velocities of the 4 stakes (Fig. 1) prior to the break-off. The assocated derived surface velocities are computed taking the surface displacements interpolated on regular time step and smoothed on 5 points. Note that Stakes 13 and 14 have more than 2 years of nearly continuous measurements, the position of Stake 13 having been measured up to the final break-off event on 29 September. The accuracy of the measurements was less than a centimeter (Faillettaz et al., 2008). Note that this constitutes a unique dataset not only because of the great accuracy and long measurement period but also due to available surface displacement measurements up to a few hours prior to the break-off event. Whereas the motion of Stake 4 is constant (Fig. 2), the three other prisms show a clear acceleration prior to break-off.

3.1 Previous findings on cold glacier break-off

These observations exhibit striking qualitative analogies with those of the 2005 Weisshorn event (Faillettaz et al., 2008).

1. This steep cold hanging glacier experiences periodic break-off events.
2. The geometrical configuration of the glacier is similar before each break-off.
3. An upper crevasse spanning the whole glacier marks a clear distinction between a stable upper part (where Stake 4 is located) and a downstream unstable part (where the other reflectors were located, Fig. 3). A crude estimation of the volume of the unstable part is thus possible.
4. Downstream this crevasse, surface displacements experience a typical acceleration prior break-off, whereas upstream this crevasse constant velocities are recorded (Stake 4 in Fig. 2).

TCD
9, 4925–4948, 2015

Prediction of glacier break-off

J. Faillettaz et al.

5. The rupture did not occur at the ice/bedrock contact but a few meters above it, within the ice (Fig. 1).

6. The total break-off occurred on two occasions; a minor side section of the glacier was released first.

Based on a retrospective analysis, the main conclusion drawn by Flotron (1977) and Röthlisberger (1981) was that the forecast of a break-off occurrence was possible using surface displacements alone. The principle is to fit the characteristic acceleration of the surface displacements with a power law behavior of the form:

$$s(t) = s_0 + u_s t - a(t_c - t)^{\theta}, \qquad (1)$$

where $s(t)$ is the displacement (in meters) at time t (in days), s_0 a constant in meters, u_s the constant velocity of the upstream part (in $\mathrm{m\,d^{-1}}$), t_c the critical time (in days), $\theta < 0$ (without units) and a (in $\mathrm{m\,d^{-\theta}}$) the parameters characterizing the acceleration. In this way, the critical time t_c, i.e., time at which the theoretical displacement becomes infinite, could be evaluated simply using such empirical law. Although break-off would necessarily occur earlier, this critical time represents the upper limit of the break-off timing.

Moreover, an oscillating pattern superimposed on the power law acceleration of the surface displacements was evidenced prior to the 2005 Weisshorn event (Pralong et al., 2005; Faillettaz et al., 2008). Such behavior was shown to be log-periodic oscillating behavior superimposed on this acceleration (for appearance and interpretation see Faillettaz et al., 2015). The time evolution of the surface displacement measurements can be described with the following equation (after Sornette and Sammis, 1995; Pralong et al., 2005):

$$s(t) = s_0 + u_s t - a(t_c - t)^{\theta}\left[1 + C\sin\left(2\pi\frac{\ln(t_c - t)}{\ln(\lambda)} + D\right)\right], \qquad (2)$$

Discussion Paper | Discussion Paper | Discussion Paper | Discussion Paper |

TCD

9, 4925–4948, 2015

Prediction of glacier break-off

J. Faillettaz et al.

where C the relative amplitude (without units), λ the logarithmic frequency (in days) and D the phase shift of the log-periodic oscillation (without units).

Note that such oscillating behavior was also evident prior to the 2014 Whymper glacier break-off, as such oscillating patterns are clearly visible on the derived velocity without post-processing (Fig. 3).

3.2 Application to forecasting

Previous findings were applied in order to forecast the break-off in real time. As soon as a significant increase in velocity was detected, the same procedure was followed as in Faillettaz et al. (2008). We periodically fitted surface displacements of all stakes to a power law (Eq. 1) and a log periodic oscillating behavior (Eq. 2). Figure 4 shows the residuals to the power law fit for two points (Stakes 13 and 14) using the last month of data to 16 September; Table 1 contains the values of the parameters in Eq. (2), taking $\lambda = 2$ d. Note that measurements are available up to the final break-off for 3 prisms (i.e., Stake 13, Stake 2 and Stake 4) and stopped on 16 September for Stake 14, i.e., 8 days before the first break-off. It appears that the power law describes well the surface displacements with an accuracy of about 5 cm, about the same order of magnitude as the one observed during the 2005 Weisshorn event. However, residuals show an oscillating pattern. When using the log-periodic function (Eq. 2), the fit (shown in red) becomes significantly better, with an accuracy of the order of magnitude of the measurement accuracy (less than a centimeter). Results show that the critical time ranges between 1 and 4 October, which is fairly close to the observed break-off.

However, even if Stake 14 is located on a section that broke off earlier, no significant differences could be detected. Our approach is not able to detect whether the break-off would happen all at once or could occur as successive small break-offs.

Now when investigating the entire dataset for Stake 13 (where measurements were performed up to the break-off) using the same method, it appears that the amplitudes of oscillations become even larger close to the break-off -that is, they reach up to 40 cm

TCD
9, 4925–4948, 2015

Title Page
Abstract Introduction
Conclusions References
Tables Figures
◀| |▶
◀ ▶
Back Close
Full Screen / Esc
Printer-friendly Version
Interactive Discussion

(Fig. 5)! Such a broad oscillating pattern had never been observed before, confirming that the jerky motion of the glacier (with oscillating nature) has a physical origin.

4 Discussion

4.1 Appearance of log-periodic behavior

Faillettaz et al. (2011a, 2015) explain the origin of the log-periodic oscillating behavior as the result of a Discrete Scale Invariance, a weaker kind of scale invariance according to which the system obeys scale invariance only at a specific scaling factor scale (Sornette and Sammis, 1995; Sornette, 1998; Zhou and Sornette, 2002a; Sornette, 2006). This partial breaking of the continuous symmetry is a result of the dynamic interactions between newly developed micro-cracks, as shown by Huang et al. (1997) and Sahimi and Arbabi (1996).

To identify the log-frequency, we analyzed the data in the same way as Faillettaz et al. (2008) with a Lomb periodogram analysis (Press, 1996; Zhou and Sornette, 2002b), which is designed to analyze non-uniformly sampled time series. This method enables us to determine f_{Lomb} as a function of $\cos(2\pi f_{\mathrm{Lomb}} t)$. The parameter λ in Eq. (2) can then be evaluated easily as $\lambda = e^{1/f_{\mathrm{Lomb}}}$. Unfortunately, the critical time t_c has to be known to perform this analysis, i.e., this analysis can only be an a posteriori analysis. It clearly shows (Fig. 6a) peaks in Lomb power (power spectral density) at $\lambda \sim 2$ d for the three analyzed points, confirming that the oscillating behavior is not a measurement artefact but has physical origins, such as the merge of newly developed micro-cracks. Note that another strong log frequency appears at $\lambda \sim 7.4$ d for Stakes 2 and 13 (Fig. 6b), after the first break-off. The reason for the appearance of such peak is not clear but is probably induced by the occurrence of the first break-off that changes the geometry of the glacier: Using experimental data, Moura et al. (2005, 2006) suggested that grain size and loading rate directly influence log-periodic oscillations. A possible explanation would thus be that the first release led to a sudden change in the global

TCD
9, 4925–4948, 2015

loading of the remaining section of the glacier, i.e., loading rate change, introducing then another subharmonic log frequency and perturbing the overall behavior of the remaining section of the glacier where Stakes 2 and 13 stand.

4.2 Power law vs. log-periodic

Besides a more accurate fit (Figs. 4 and 5), Fig. 7 (bottom) shows that errors (given as 95 % confidence interval) in the determination of the critical time t_c are generally smaller for log-periodic fit than power law fit, confirming once again a more reliable log-periodic fit. Usually power law evaluates a larger (later) critical time than log-periodic law.

4.3 Accurate determination of break-off occurrence

As critical time t_c given by power law or log-periodic fit indicates time at which surface displacements are theoretically infinite, real break-off is expected before t_c. When fitting in real time the surface displacement with both power law and log-periodic behavior, it is not only possible to assess the critical time but also the time at which the derived velocities are expected to reach a given threshold (for example $50\,\mathrm{cm\,d^{-1}}$ or $1\,\mathrm{m\,d^{-1}}$). Fitting and estimating the time at which the associated velocity reaches a given threshold provides a more accurate way to predict the real break-off. We developed a software based on this idea by fitting in real time the measurements with both power law and log-periodic behavior and thus provide an estimate of the break-off time.

From our knowledge, it is not possible to know in advance the velocity at which break-off will occur. However, from previous events (Weisshorn 1973 and 2005 event, Flotron, 1977; Röthlisberger, 1981; Faillettaz et al., 2008), it seems that break-off occurs between $50\,\mathrm{cm\,d^{-1}}$ to $1.2\,\mathrm{m\,d^{-1}}$, but this is based on a restricted number of events.

Taking threshold surface velocities of $50\,\mathrm{cm\,d^{-1}}$ and $1\,\mathrm{m\,d^{-1}}$, our analysis performed every days from the 12 to 16 September suggested that break-off could occur between the 23 September ($v_{th} = 50\,\mathrm{cm\,d^{-1}}$) and the 29 September ($v_{th} = 1\,\mathrm{m\,d^{-1}}$). Note that this

TCD
9, 4925–4948, 2015

method provided the exact timing of the real break-offs, around 10 days in advance. Following this analysis, alert was immediately sent to the authorities leading them to close the endangered area one week before the event. Note that the definition of the velocity threshold has an influence on the prediction itself, as we saw nearly one week is needed for the glacier to accelerate from $50\,\mathrm{cm\,d^{-1}}$ to $1\,\mathrm{m\,d^{-1}}$. The precise prediction would also not only be based on a correct fit of the surface displacement data but also on a guess of this parameter. We suggest to choose $40\,\mathrm{cm\,d^{-1}}$ as a conservative threshold to define a high break-off danger time zone.

4.4 How much in advance can be the break-off predicted?

Surface displacement was analyzed retrospectively based on the last month of data for each prism, and the critical time as well as the time at which the fitted velocity reached $50\,\mathrm{cm\,d^{-1}}$ (v_{50}) and $1\,\mathrm{m\,d^{-1}}$ (v_{100}) were plotted as a function of the time of analysis (Fig. 7). Associated errors (Fig. 7 bottom) account for the fitting procedure.

First, the prediction is better using log-periodic fit than power law fit. This retrospective analysis shows that the prediction is correct after 12 September, i.e., 11 and 17 days before the break-off with a confidence interval becoming less than than 10 days for log-periodic fit.

This analysis points out the great prediction potential – and early warning perspectives – of this method, as the exact time of the break-off could be forecast almost 2 weeks before its occurrence. Note that both power law and log-periodic fits become less accurate after the first break-off for Stake 13. Such effect might be related to the sudden change in glacier geometry that may influence surface displacements at Stake 13. However, note that time at which estimated derived velocity reaches $1\,\mathrm{m\,d^{-1}}$ (v_{100}) is stable, still pointing at 29 September.

TCD
9, 4925–4948, 2015

5 Conclusions

Grandes Jorasses glacier broke off twice, on 23 and 29 September 2014. In 2008, as it was suspected that this glacier becoming unstable, a long-term monitoring program was initiated. At the time of the break-off, 4 prisms spread over the glacier enabled surface displacements to be measured in a very accurate way up to the time of the break-off. By regularly analyzing the dataset, it was possible to forecast the event ten days in advance, enabling local authorities to close off the endangered areas and thus prevent catastrophic outcomes.

It was possible to confirm definitely that surface displacement exhibits strong log-periodic oscillating behavior superimposed on a global power law acceleration prior to its break-off, as first discovered for the Weisshorn event (Faillettaz et al., 2015). In the immediate vicinity of the break-off, such oscillations reached an amplitude of more than 40 cm, almost one order of magnitude larger than revealed in previous findings. By fitting surface displacements to this behavior, the critical time, i.e. time at which surface displacement become infinite, can be determined. The surface velocities at the two events were 0.5 and 1.2 $\mathrm{m\,d^{-1}}$, in the same range as for the Weisshorn event, suggesting that break-off of a cold hanging glacier could occur as soon as surface velocities reached 0.5 $\mathrm{m\,d^{-1}}$. By taking critical time as an upper time bound of the event occurrence, this method provides a good estimate of the timing of the break-off. We showed that evaluating the time at which extrapolated velocities (based on the log-periodic fit) reach a given threshold (0.5 and 1 $\mathrm{m\,d^{-1}}$) provides a significantly better forecast. However, in the present case, the time needed for the glacier to increase its velocity by 50 to 100 $\mathrm{cm\,d^{-1}}$ was in the order of a week. In practice, we suggest that $v = 0.4\,\mathrm{m\,d^{-1}}$ be applied to determine the period of highly probable break-off occurrence. A retrospective analysis based on this method showed that an accurate prediction of the phenomenon can be made two weeks before its occurrence using the last month of surface displacement data and 0.5 and 1 $\mathrm{m\,d^{-1}}$ as velocity thresholds. Although the crude volume can be estimated, provided that a sufficient number of measurements points is available,

TCD
9, 4925–4948, 2015

this method does not seem to be able to detect whether the break-off will occur as a single large event or as a series of smaller events, as no differences in the evolution of surface displacements were detected. This has of course important consequences for risk evaluation, as the resulting ice avalanche (and also the chain of processes resulting from its release) depends on the initial ice volume released. To conclude, our results suggest that the present methods exploiting the log-periodic oscillating behavior are universal and thus can be applied in real time to forecast a break-off on any cold unstable hanging glacier.

Acknowledgements. The authors thank Susan Braun-Clarke for proofreading the English.

References

Faillettaz, J., Pralong, A., Funk, M., and Deichmann, N.: Evidence of log-periodic oscillations and increasing icequake activity during the breaking-off of large ice masses, J. Glaciol., 54, 725–737, doi:10.3189/002214308786570845, 2008. 4927, 4930, 4931, 4932, 4933, 4934, 4935

Faillettaz, J., Funk, M., and Sornette, D.: Icequakes coupled with surface displacements for predicting glacier break-off, J. Glaciol., 57, 453–460, doi:10.3189/002214311796905668, 2011a. 4927, 4934

Faillettaz, J., Sornette, D., and Funk, M.: Numerical modeling of a gravity-driven instability of a cold hanging glacier: reanalysis of the 1895 break-off of Altelsgletscher, Switzerland, J. Glaciol., 57, 817–831, doi:10.3189/002214311798043852, 2011b. 4927

Faillettaz, J., Funk, M., and Sornette, D.: Instabilities on Alpine temperate glaciers: new insights arising from the numerical modelling of Allalingletscher (Valais, Switzerland), Nat. Hazards Earth Syst. Sci., 12, 2977–2991, doi:10.5194/nhess-12-2977-2012, 2012. 4927

Faillettaz, J., Funk, M., and Vincent, C.: Avalanching glacier instabilities: review on processes and early warning perspectives, Rev. Geophys., 53, 203–224, doi:10.1002/2014RG000466, 2015. 4927, 4932, 4934, 4937

Flotron, A.: Movement studies on hanging glaciers in relation with an ice avalanche, J. Glaciol., 19, 671–672, 1977. 4932, 4935

Huang, Y., Ouillon, G., Saleur, H., and Sornette, D.: Spontaneous generation of discrete scale invariance in growth models, Phys. Rev. E, 55, 6433–6447, doi:10.1103/PhysRevE.55.6433, 1997. 4934

Margreth, S., Faillettaz, J., Funk, M., Vagliasindi, M., Diotri, F., and Broccolato, M.: Safety concept for hazards caused by ice avalanches from Whymper hanging glacier in the Mont-Blanc massif., Cold Reg. Sci. Technol., 69, 194–201, doi:10.1016/j.coldregions.2011.03.006, 2011. 4930

Moura, A., Lei, X., and Nishisawa, O.: Prediction scheme for the catastrophic failure of highly loaded brittle materials or rocks, J. Mech. Phys. Solids, 53, 2435–2455, doi:10.1016/j.jmps.2005.06.004, 2005. 4934

Moura, A., Lei, X., and Nishisawa, O.: Self-similarity in rock cracking and related complex critical exponents, J. Mech. Phys. Solids, 54, 2544–2553, doi:10.1016/j.jmps.2006.06.010, 2006. 4934

Pralong, A. and Funk, M.: On the instability of avalanching glaciers, J. Glaciol., 52, 31–48, doi:10.3189/172756506781828980, 2006. 4927

Pralong, A., Birrer, C., Stahel, W. A., and Funk, M.: On the predictability of ice avalanches, Nonlinear Proc. Geoph., 12, 849–861, doi:10.5194/npg-12-849-2005, 2005. 4932

Press, W.: Numerical Recipes in Fortran 90: Volume 2, Volume 2 of Fortran Numerical Recipes: The Art of Parallel Scientific Computing, Fortran numerical recipes, Cambridge University Press, Cambridge, available at: http://books.google.ch/books?id=SPEi4mCfhacC, 1996. 4934

Röthlisberger, H.: Eislawinen und Ausbrüche von Gletscherseen, in: Gletscher und Klima – Glaciers et Climat, Jahrbuch der Schweizerischen Naturforschenden Gesellschaft, wissenschaftlicher Teil 1978, edited by: P. Kasser, Birkhäuser Verlag Basel, Boston, Stuttgart, 170–212, 1981. 4932, 4935

Sahimi, M. and Arbabi, S.: Scaling laws for fracture of heterogeneous materials and rock, Phys. Rev. Lett., 77, 3689–3692, doi:10.1103/PhysRevLett.77.3689, 1996. 4934

Sornette, D.: Discrete-scale invariance and complex dimensions, Phys. Rep., 297, 239–270, doi:10.1016/S0370-1573(97)00076-8, 1998. 4934

Sornette, D.: Critical Phenomena in Natural Sciences: Chaos, Fractals, Selforganization and Disorder: Concepts and Tools, Springer Series in Synergetics, Springer, Berlin, available at: http://books.google.com.au/books?id=uYHQHV2hCpwC, 2006. 4934

Sornette, D. and Sammis, C. G.: Complex critical exponents from renormalization group theory of earthquakes: implications for earthquake predictions, J. Phys. I, 5, 607–619, doi:10.1051/jp1:1995154, 1995. 4932, 4934

Zhou, W.-X. and Sornette, D.: Generalized q analysis of log-periodicity: applications to critical ruptures, Phys. Rev. E, 66, 046111, doi:10.1103/PhysRevE.66.046111, 2002a. 4934

Zhou, W.-X. and Sornette, D.: Evidence of intermittent cascades from discrete hierarchical dissipation in turbulence, Physica D, 165, 94–125, doi:10.1016/S0167-2789(02)00390-1, 2002b. 4934

TCD

9, 4925–4948, 2015

Prediction of glacier break-off

J. Faillettaz et al.

Table 1. Values of the estimated coefficients of Eq. (2) with $\lambda = 2$ d and the root-mean-square error (RMSE) of the fit, first two columns corresponding to the parameters of the fit used in Fig. 4 for the period 16.08–16.09, last two columns corresponding to the parameters of the fit used in Fig. 5 for the period 30.08–30.09. t_c is given in days after the first days of the investigated period.

Parameter	Units	Stake 13 (up to 16 Sep)	Stake 14 (up to 16 Sep)	Stake 13 (up to 29 Sep)	Stake 2 (up to 29 Sep)
t_c	d	45.23	48.93	41.76	44.18
	date	1 Oct 2014 5 a.m.	4 Oct 2014 10 p.m.	10 Oct 2014 6 p.m.	13 Oct 2014 4 a.m.
θ	–	−0.21	−0.48	−1.04	−1.50
s_0	m	-1.86×10^4	-1.83×10^4	-2.52×10^4	-1.49×10^4
u_s	$\mathrm{m\,d^{-1}}$	2.53×10^{-2}	2.48×10^{-2}	3.43×10^{-2}	2.02×10^{-2}
a	$\mathrm{m\,d^{-\theta}}$	25.41	33.12	1 466.22	569.29
C	–	2.68×10^{-3}	5.75×10^{-3}	3.27×10^{-2}	3.49×10^{-2}
D	–	2.90	1.46	2.26×10^{-5}	11.9
RMSE	$\mathrm{m\,d^{-1}\,m^{-1}}$	8.7×10^{-3}	8.4×10^{-3}	3.14×10^{-2}	1.62×10^{-2}

TCD
9, 4925–4948, 2015

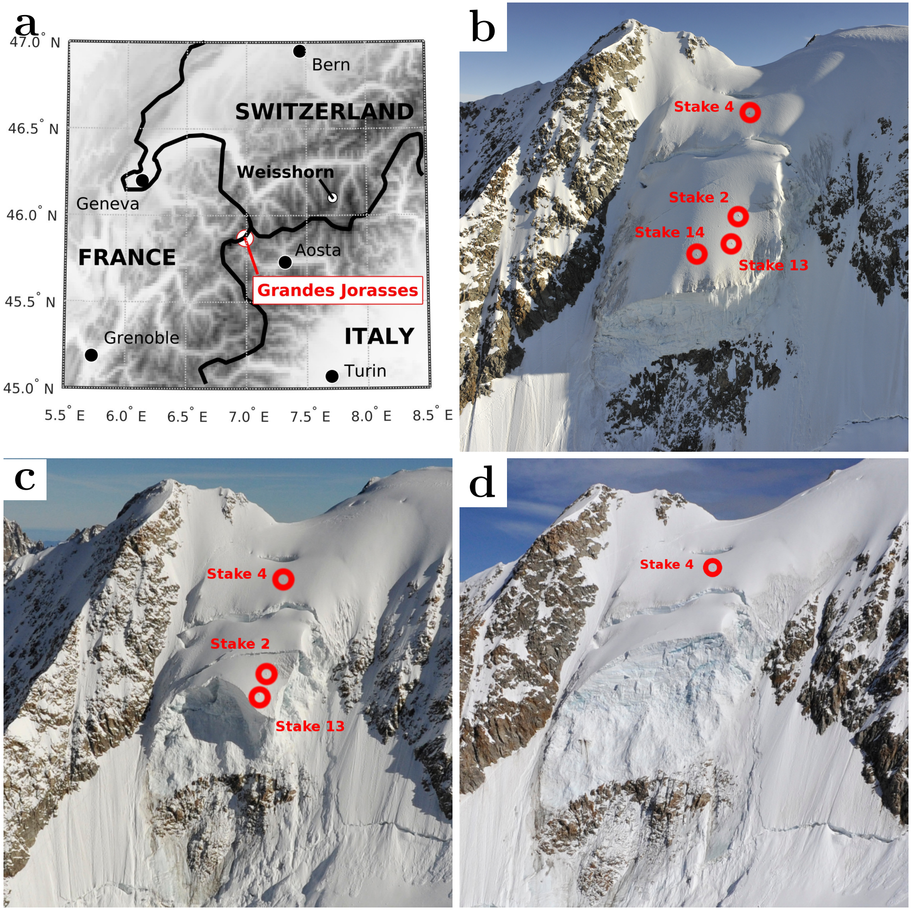

Figure 1. (a) Geographical situation of the studied glacier. **(b)** Grandes Jorasses (Whymper) glacier before (23 August 2014), **(c)** after the first break-off (23 September 2014) and **(d)** after the second break-off (30 September 2014).

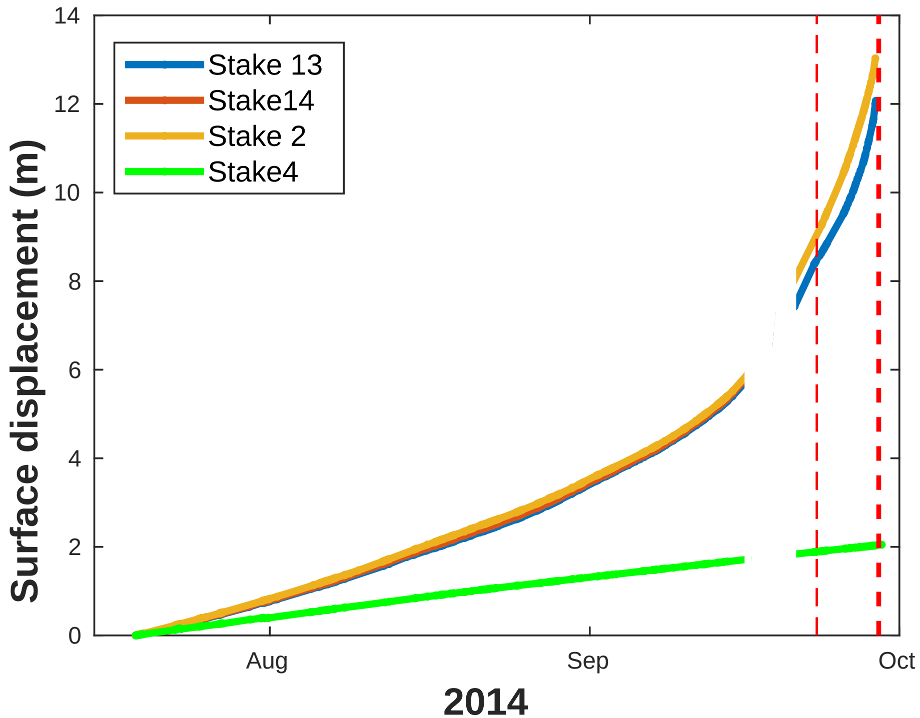

Figure 2. Surface displacement of the 4 stakes before the break-off using 19 July 2014 as reference (when Stake 2 and Stake 4 were installed). Vertical red dashed lines indicate the occurrence of the two break-offs, on 23 and 29 September 2014. Interrupted lines indicate a period of bad weather conditions without measurements. Note that Stake 14 was not surveyed after 16 September 2014, i.e., one week before the first break-off.

TCD
9, 4925–4948, 2015

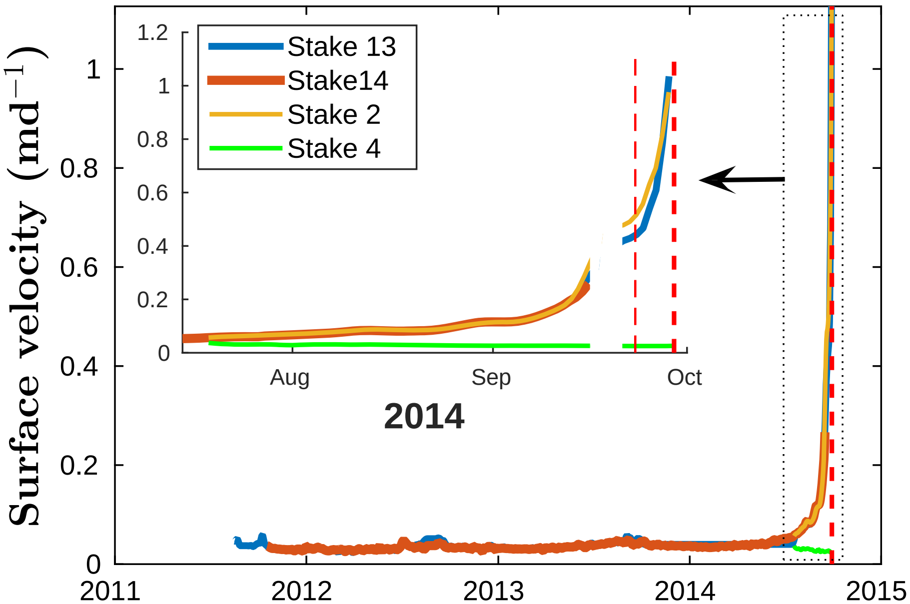

Figure 3. Smoothed surface velocity of the 4 stakes since 2012. Inset shows a closer view during the same period as that in Fig. 2.

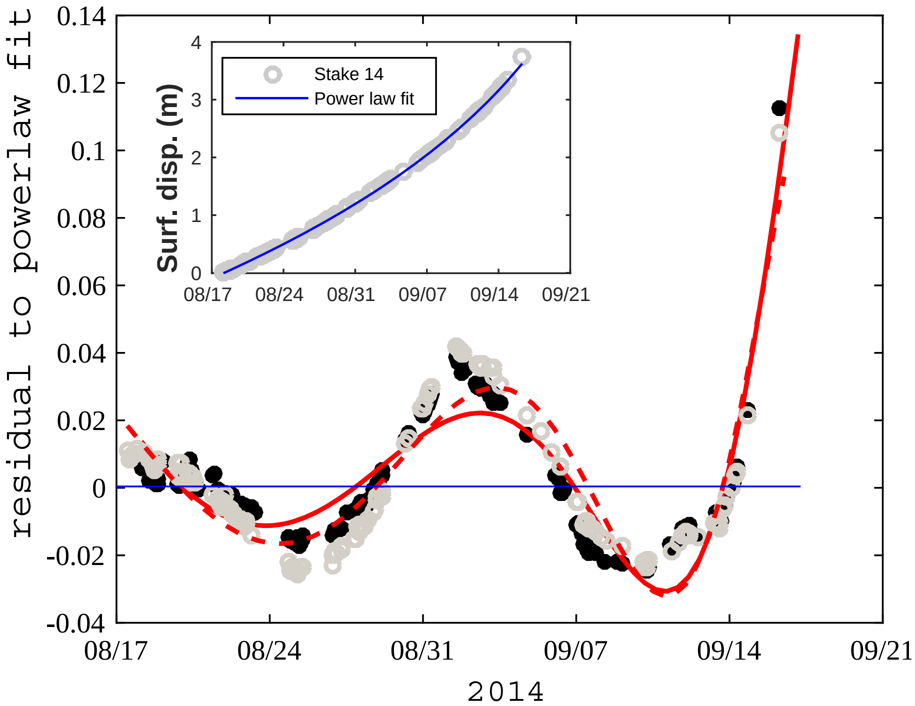

Figure 4. Residuals (in meters) to the power law fit (in blue) for the period 17 August–17 September (last measurement of Stake 14) for both Stake 13 (black points) and Stake 14 (gray circles) and associated log-periodic fit (solid line for Stake 13 and dashed line for Stake 14). Values for the parameters are shown in Table 1. Inset shows the surface displacement (gray) and power law fit (blue) at Stake 14.

TCD
9, 4925–4948, 2015

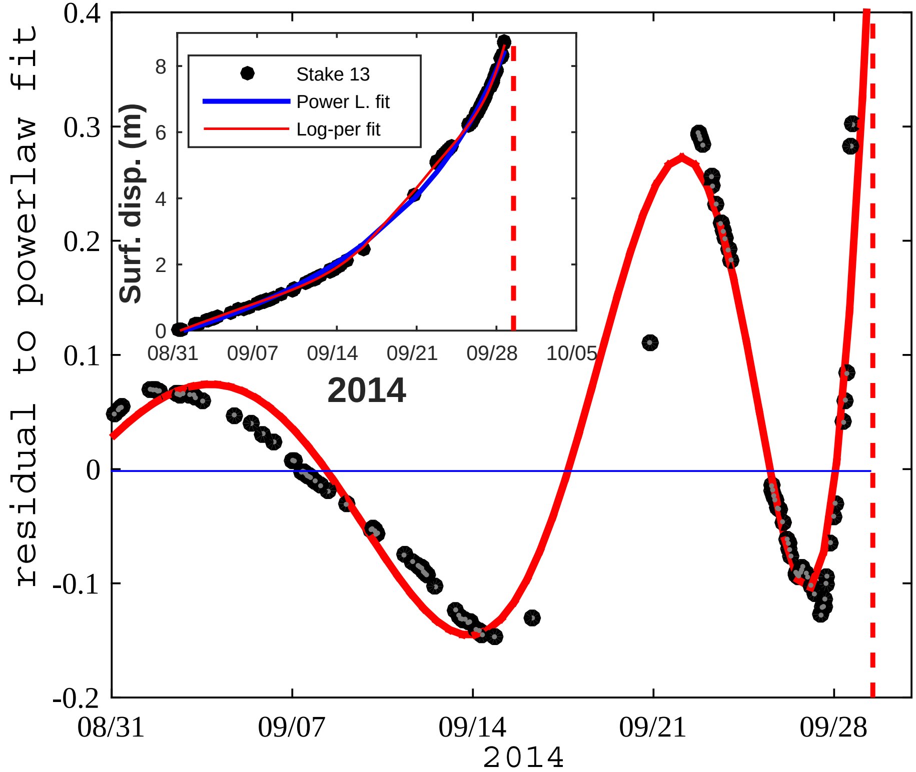

Figure 5. Residuals (in meters) to the power law fit (black point) and log-periodic fit (red line) for Stake 13 based on the last month of data prior to the break-off. Values of the parameters are shown in Table 1.

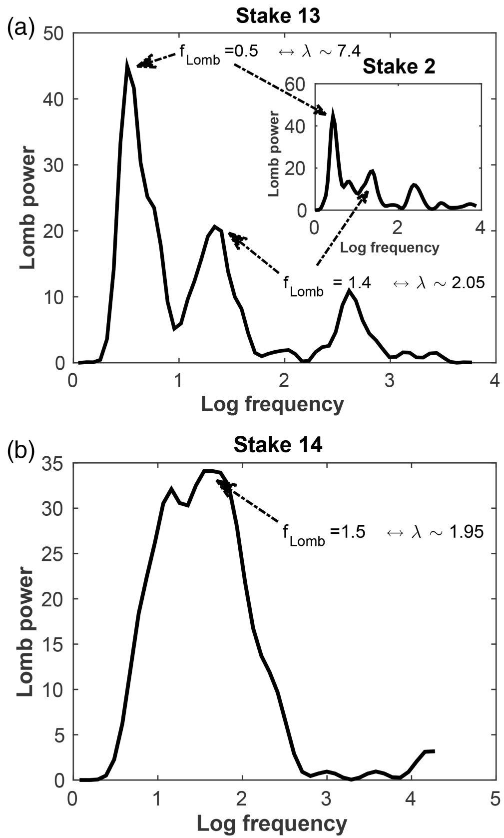

Figure 6. (a) Lomb periodogram for Stakes 13 and 2 (in inset) as well as the corresponding log frequencies (λ) of the peaks. **(b)** Lomb periodogram for Stake 14 as well as the corresponding log frequencies (λ) of the peaks.

TCD
9, 4925–4948, 2015

Prediction of glacier break-off

J. Faillettaz et al.

Title Page
Abstract Introduction
Conclusions References
Tables Figures
◄ ►
◄ ►
Back Close
Full Screen / Esc
Printer-friendly Version
Interactive Discussion

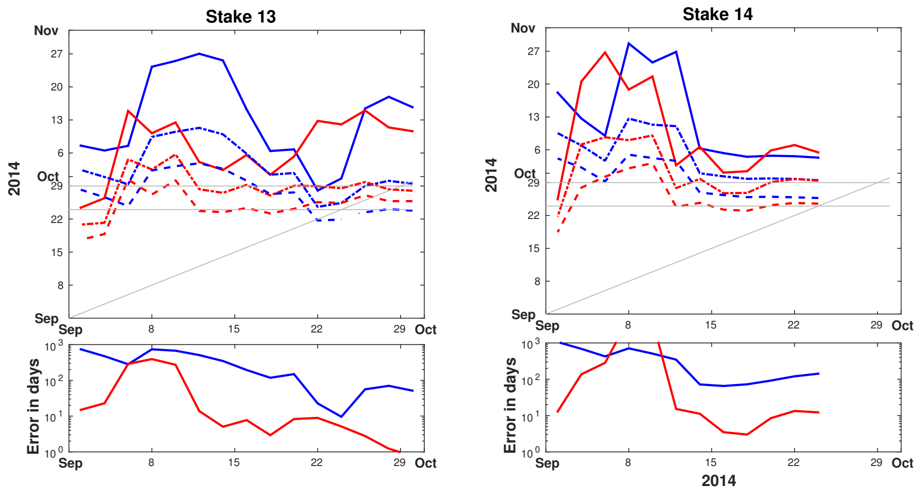

Figure 7. Top: Thick lines: evaluated critical time t_c for power law (blue) and log-periodic (red) fit for Stakes 13 (left) and 14 (right) as a function of the time of analysis. Interrupted lines indicate time at which estimated derived velocity from power law and log-periodic fit reaches $50\,\mathrm{cm\,d^{-1}}$ (dashed lines, v_{50}) and $1\,\mathrm{m\,d^{-1}}$ (dot-dash line, v_{100}). Horizontal grey lines represent the observed break-off (23 and 29 September), inclined gray line indicates the time of analysis. Bottom: Error in days on critical time fitted with power law (blue) and log-periodic (red) estimated from the 95 % confidence interval. Errors on v_{50} and v_{100} are similar to the errors on critical time, as they are directly derived from these fits.